



Landform-regolith mapping in the West African context

Benjamin Sawadogo, Ousmane Bamba, Dominique Chardon

► To cite this version:

Benjamin Sawadogo, Ousmane Bamba, Dominique Chardon. Landform-regolith mapping in the West African context. *Ore Geology Reviews*, 2020, 126, pp.103782. <10.1016/j.oregeorev.2020.103782>. <hal-03491584>

HAL Id: hal-03491584

<https://hal.science/hal-03491584v1>

Submitted on 17 Oct 2022

HAL is a multi-disciplinary open access archive for the deposit and dissemination of scientific research documents, whether they are published or not. The documents may come from teaching and research institutions in France or abroad, or from public or private research centers.

L'archive ouverte pluridisciplinaire **HAL**, est destinée au dépôt et à la diffusion de documents scientifiques de niveau recherche, publiés ou non, émanant des établissements d'enseignement et de recherche français ou étrangers, des laboratoires publics ou privés.



Distributed under a Creative Commons CC BY-NC 4.0 - Attribution - Non-commercial use - International License

Landform-regolith mapping in the West African context

Benjamin Sawadogo^{a,b}, Ousmane Bamba^a, Dominique Chardon^{a,b,c*}

^aDépartement des Sciences de la Terre, Université Joseph Ki-Zerbo,

Ouagadougou, Burkina Faso

^bIRD, Ouagadougou, Burkina Faso

^cGET, Université de Toulouse, CNRS, IRD, UPS, France.

Submitted to ***Ore Geology Reviews***, 30 March 2020

Revised 8 June 2020

Revised 22 July 2020

Revised 10 September 2020

***Corresponding author**

E-mail address: dominique.chardon@ird.fr

24 **HIGHLIGHTS**

- 25 - Presentation of a landform-regolith mapping protocol adapted to West Africa
- 26 - Landform-regolith map transposed into a soil prospectivity map
- 27 - Implications for exploration strategies
- 28 - Applicability to the rest of West Africa and inter-tropical mineral provinces

29

30 **Abstract**

31 In this paper, we present an integrated landform-regolith mapping protocol/chart for
32 West Africa developed using a case from Central Burkina Faso. The chart accounts for
33 (i) the specificities of the ubiquitous, duricrust-capped remnants of the regional
34 paleolandsurfaces - particularly the residual or detrital character of the Fe duricrusts –
35 and (ii) the diversity of the remaining, non-duricrusted portions of the landscape, with
36 an emphasis on the pitfalls encountered in determining the in-situ or transported
37 character of the regolith. The paper also provides field identification criteria and
38 illustrations of the typical West African landform-regolith associations. The landform-
39 regolith mapping chart is integrated into a prospectivity chart, which is used to define
40 exploration guides: (ii) defining sampling strategies, (ii) interpreting potential
41 geochemical anomalies and (iii) targeting lateral extensions of known bedrock
42 mineralizations. The mapping protocol further allows for the definition of a class of
43 landform-regolith associations propitious to supergene mineral concentrations. The
44 mapping protocol is shown to be transposable to wetter contexts and, more generally,
45 to other tropical shield provinces.

46

keywords: Pediment, Weathering profile, Duricrust, Detrital duricrust, Mineral

exploration

1. Introduction

Regolith cover is often an obstacle to mineral exploration in the tropics because of poor or uneven outcrop conditions of the geological substrate. Exploration relies on sampling of surface material (soil, lag, duricrust, or even termite mounds or vegetation) to detect geochemical anomalies resulting from the geochemical dispersion of a primary bedrock mineralization through the regolith. However, interpretation of a surface geochemical anomaly depends on the nature and the history of the regolith. The regolith may occur in situ on the rocks from which it derives by weathering or may have been transported and re-weathered. The main challenges for geochemical exploration are therefore to (i) choose the appropriate spatial density, depth and technique of sampling, (ii) identify the right regolith material to sample and (iii) interpret geochemical anomalies (Anand and Butt, 2010). Landform-regolith mapping is therefore a crucial prerequisite to mineral exploration in the tropics. Several mapping protocols have been developed in the last decades (Butt, 2016), the most popular being derived from, or comparable to, the RED model (Anand et al., 1993; Anand and Butt, 2010). That model categorizes the landscape into 3 regolith-landform regimes: relict (R, for lateritic residuum), erosional (E, for erosional plains and steep slopes) and depositional (D, sediments masking the weathering profile or the bedrock). RED-type models were applied (or slightly adapted) in sub Saharan West Africa (e.g., Zeegers and Lecomte, 1992; Arhin et al., 2015; Butt, 2016). While implicitly or explicitly referring to RED-type models, most authors and exploration geologists categorize the ubiquitous

Al-Fe duricrust cover of West Africa as lateritic residuum (i.e., duricrusts are the ultimate residual term of weathering, topping a weathering profile derived from the underlying bedrock) (e.g., Boeglin and Mazaltarim, 1989; Roquin et al., 1990; Zeegers and Lecomte, 1992; Howell et al., 1996; Tardy, 1997; Freyssinet et al., 2005; see Butt and Bristow, 2013). However, most (>80%) part of West Africa is occupied by pediments capped by detrital Fe-duricrusts or unconsolidated detrital sediments (Chardon et al., 2018; see also Bolster, 1999; Butt and Bristow, 2013). These pediments are inherited from 3 Neogene paleolandscape stages of the well documented regional morphoclimatic sequence (Fig.1). The ubiquity of paleo- and active pediment systems in West Africa therefore prompts the reevaluation of landform-regolith mapping protocols.

Here we present an integrative landform-regolith mapping chart for West Africa based on the case presented in this paper. We aim at providing geomorphologists, geologists, geochemists and the mineral exploration community with field documentation, identification criteria and illustrations of the typical landforms and regolith. The chart accounts for the specificities of the remnants of the regional morphoclimatic sequence (Fig. 1) - particularly the residual or detrital character of the Fe duricrusts – and the remaining, non-duricrusted portions of the landscape. We show how the resulting landform-regolith map is converted into a soil prospectivity map, which is used for (i) defining sampling strategies, (ii) interpreting potential geochemical anomalies and (iii) targeting lateral extensions of known deposits. The mapping protocol is shown to be applicable to wetter contexts and, more generally, to other tropical shield provinces.

2. Context and method

Our study is based on a regolith mapping project of part of the Goren greenstone belt in North-Central Burkina Faso, in the semi-arid Soudanian climatic zone (Fig. 2). The study area is typical of the greenstone-hosted gold deposits of the Eburnean orogen of the southern West African craton (e.g., Milési et al., 1992; Fig. 2). The belt is the richest in Burkina Faso in terms of gold indices and prospectivity (Castaing et al., 2003). The mapping protocol is illustrated on a typical 7 x 6 km extract (Figs. 3 and 4) of a larger mapped area (26 x 15 km) that allowed for a comprehensive inventory of the spatial diversity of the regolith covers. The geological substrate comprises a typical Birimian greenstone association of low-grade schistose volcanosediments (sandstone-pelite associations interlayered with mafic and felsic volcanics) and metabasic rocks (gabbro, diorite and andesite) (Fig. 3).

For landform-regolith mapping, we used a 1:10 000 scale, 1-m contour base map derived from a smoothed Lidar digital elevation model (e.g., Figs. 3 and 4). Mapping was undertaken along a number of itineraries throughout the landscape (Fig. 3) complemented by photointerpretation that allowed refinement of various map units. Field mapping consisted mostly of (1) landscape interpretations and establishment of landscape chronologies, (2) description and identification of the duricrust-capped remnants of the West African morphoclimatic sequence (Fig. 1), (3) description and classification of the geomorphology and regolith cover of the erosional landforms separating the duricrust-capped remnants and (4) description and classification of the material being actively remobilized by mechanical erosion and transport.

Through comprehensive field investigation the definition of 20 landform-regolith association map units (section 3; Fig. 4) was established. These units may be grouped into 4 main categories on the basis of the nature/degree of genetic link

between the material exposed at the surface and the underlying geological substrate (section 4). This categorization has implication on the intensity of expression of a geochemical anomaly through the regolith that is related to the underlying bedrock mineralization, the occurrence of “transported” anomalies in the regolith or the potential occurrences of bedrock anomalies masked by the regolith.

3. Landform-regolith associations

3.1. Upper paleolandsurfaces

3. 1. 1. Bauxitic (African) paleolandsurface (1BxD)

It is preserved as 120- to 150-m high, duricrust-capped plateaus that are flat or slightly convex, with less than 25 m of elevation amplitude for a single plateau (Fig. 6a and 6b). In the study area, the largest plateau is 1 km long and 40 m wide (Fig. 4). The weathering profile underlying the bauxitic duricrust is 50- to 100-m thick (thickest on mafic rocks). It is observed on the steep sides of plateaus, whose edge consists of a scarp made in the duricrust. The profile consists mainly of a kaolinite rich saprolite underlying a 5 to 10 m thick duricrust. Saprolite is absent on quartzite and silicified volcanosediments, so that the duricrust rests directly on saprock. Duricrusts are of two main types: bauxites, that are massive or breccia-like (Fig. 7a to 7d), and Fe bauxites, that are nodular or pisolitic (Fig. 7e and 7f). Breccia-like bauxites are more common on volcanosedimentary substrate and massive bauxites are equally found on mafic rocks and volcanosediments. Fe bauxites are degraded bauxites enriched in iron (e.g., Boulangé, 1986, 1984) and mostly found on the lowermost portions of wide plateaus.

3. 1. 2. Intermediate paleolandsurface (2InD, 2InC, 2InR)

Relics of that paleolandsurface occur as two duricrust-capped geomorphological types. The most common type (1) is smooth hilly slopes or ridges sloping away from bauxitic plateaus (Fig. 4, Fig. 5 and Fig. 6b). They are stepped under the bauxitic plateaus (most of the time 50 m under the plateau edge) and, in some cases, attached to it in such a way that there is continuity between the Bauxitic and Intermediate duricrusts. The downslope topographic profile of the relics or their surface envelope is convexo-concave to convex. Relics have 50 to 500 m of across-slope width, with a slope ranging from 5 to 20 % and an elevation amplitude of 20 to 75 m. Type 2 relics are 50- to 500-m-wide isolated plateaus that dominate the lowland by 15 to 60 m (Fig. 6c). Plateaus are inclined (4 to 10 % slope), with an individual elevation amplitude of 10 to 30 m. The disposition and the distribution and slope of type 2 plateaus indicate that the Intermediate paleolandsurface radiated as wide piedmonts around the Bauxite-bearing topographic massifs and that type 1 relics represent upslope portions of these piedmonts. The hilly morphology of type 1 relics appears to result from the collapse of the paleolandsurface by mass wasting after its abandonment by relief inversion. The Intermediate weathering profile comprises a 10 to 50 m thick saprolite horizon, a carapace (that can be more than 10 m thick) and a topping duricrust (5-10 m thick for type 1 and 2-5 m thick for type 2 geomorphological occurrences).

Relics of the Intermediate paleolandsurface are mapped as 3 landform-regolith associations. The first one (*2InD*) is the original duricrust-capped landsurface. The duricrust found on type 1 relics is an Al-Fe duricrust, often dismantled into meter-size blocks (Fig. 8a). This duricrust consists of a mix of Fe oxyhydroxides hosting Al-Fe rich relicts (Fig. 8b) or a pack of nodules / pisoliths (Fig. 8c) recalling that of the Fe bauxites (Fig. 7e). The nodular / pisolitic Al-Fe duricrust appears to be the late result of the

weathering process that started by the reworking of the massive or breccia-like bauxite into nodular or pisolitic Fe bauxite. Besides, that type of Intermediate Al-Fe duricrust has been shown to derive from the ferruginization of an evolved bauxitic duricrust (Boulangé, 1986). This is further supported, in the present case, by the common occurrences of bauxites embedded in the Al-Fe Intermediate duricrust that have not been completely “digested” by the ferruginization process (Fig. 8d). Therefore, the duricrust covering the type 1 Intermediate ridges could be mistaken for a duricrust of the Bauxitic paleolandsurface without a careful geomorphological investigation. The duricrust capping isolated Intermediate plateaus (type 2) is a dense, dark-violet Fe duricrust (Figs. 8e and 8f). It is formed by the coalescence of Fe oxyhydroxide nodules and tubes, with a coherent interstitial matrix (less than 10% of the volume) made up mostly of Fe oxyhydroxides and kaolinite.

The second landform-regolith association related to the Intermediate paleolandsurface (*2InC*) corresponds to type 1 or 2 geomorphic occurrences that expose the carapace layer instead of the duricrust cap. This configuration results from the stripping of the duricrust or its non-development. The carapace (Fig. 9) is characteristically reddish or dark-red and friable and contains goethitic, - and, to a lesser extent, hematitic - concretions 1 to 30 cm in size. The concretions are pedorelictual and are angular, sub-angular, nodular, tubular or platy; others are cutanes. Concretions are dark-violet and some preserve bedrock fabrics. The carapace matrix is a pulverulent ochre-orange mix of clays and Fe oxyhydroxide nodules (Fig. 9). The carapace with low matrix content (Fig. 9b) should not be mistaken for the nodular Intermediate Fe duricrust (Fig. 8e) or that hosting scattered heterometric nodules (Fig. 9c) for a conglomeratic duricrust (see section 3. 2).

The third and last landform-regolith association related to the Intermediate paleolandsurface (*2InR*) results from the erosion / collapse of type 1 or 2 landscape relics and concomitant dismantling of their topping duricrust. The typical result is a residual hill covered with dispersed blocks or gravel of Intermediate duricrust. The saprolite and/or carapace layers of the weathering profile can crop out on the slopes or the crestal region of the residual hill.

3. 2. *Paleo-glacis systems*

Relics of the High and Middle glacis systems are preeminent in the landscape, as it is the case throughout West Africa and particularly on granite-greenstone terrains (e.g., Grimaud et al., 2015). These systems used to form the piedmonts of the massifs preserving relics of the upper paleolandsurfaces (Figs. 4 and 5).

3. 2. 1. *Geomorphology*

High glacis relics are inclined (4% mean slope) and very slightly concave plateaus (Figs. 10a to 10c), with upslope and downslope heights of 10-40 m and 5-15 m, respectively. They have a downslope width ranging from 50 to 700 m and rarely exceed 1km in across-slope length. Relics are not connected to the massifs anymore for a peripheral hollow (Fig. 5) formed after abandonment of the High Glacis. The duricrust capping the High glacis is a 2 to 4 m thick Fe duricrust that marks the edge (scarp) of plateaus and tops a weathering profile less than 30 m thick (Fig. 11a).

Middle glacis relics occupy the largest area of all the duricrust-capped paleolandsurfaces (Fig.4). They have lower slopes (1-3%) than those of the High glacis and form low-lying plateaus (< 5 m high) with downslope widths of up to 2 km

(Fig.10d). The middle glacia may form a continuous surface with the High glacia marked by a very subtle break of slope and (especially) a change in the thickness and nature of the capping duricrust (Fig. 10c). A comparable continuity is also very commonly observed between the Middle glacia and the Low glacia / active pediment (Fig.5). The weathering profile under the middle glacia is thin (<3 m), with a carapace-Fe duricrust layer rarely more than 1 m thick (Fig. 11b). The Fe duricrust forms a scarplet at plateau edges.

3. 2. 2. Landform-regolith associations of the High and Middle glacia systems

The typical landform-regolith association of the High glacia (*3HgD*) is a detrital Fe duricrust formed by cemented clastic material. Two common types are distinguished: (i) coarse conglomeratic (Fig. 11c), preferentially found on upper slopes of the relics and close to the high topographic massifs and (ii) finer-grained (sand-gravel granulometry; Fig. 11d) in distal parts of High glacia (i.e., closer to the main drains at the time the glacia was functional). In the first type, pebbles are angular, sub-angular, or rounded. They are mostly bauxitic and Intermediate duricrusts, vein quartz, transported Fe concretions or, more rarely, bedrock. The matrix is a mix of clay, silt, sand and gravel made of reworked saprolite, duricrust clasts, Fe oxyhydroxide nodules and clasts. In the finer-grained type, the nature of the gravel is comparable to that of the coarse conglomeratic type and the matrix does not exceed the sand granulometry. On initial field observations, the detrital nature of the fine-grained duricrust may be overlooked, with fateful implication as to whether the duricrust material formed in-situ or was transported before cementation. The duricrust-capped landform-regolith association for the Middle glacia (*4MgD*) compares to that of the High glacia (*3HgD*) although the

239 coarse conglomeratic type is found only in the uppermost portions of some glacia relics.

240 The Middle glacia Fe duricrust is detrital and has a gravel – sand granulometry. It has

241 vacuoles and is more porous than that of the High glacia (Figs 11e and 11f).

242 Areas of preserved High or Middle glacia exposing the carapace instead of the

243 duricrust have been ascribed to a distinctive association (*3HgC* and *4MgC*, respectively).

244 The High glacia carapace is scoriaceous and highly porous, light-colored (pinkish to

245 yellowish; Fig. 12). If present, Fe nodules are millimeter or centimeter in size and

246 bedrock structures can persist in the carapace, by contrast with the Intermediate

247 carapace. The carapace of the Middle glacia compares to that of the High glacia but Fe

248 concretions are scarce and most of the time invisible macroscopically. In absence of

249 bedrock structures, whether the glacia carapace was formed by weathering of the

250 underlying bedrock is difficult to assess. It may derive from cementation of fine-grained

251 detrital material.

252 Areas of preserved High or Middle glacia exposing the Intermediate carapace

253 layer are not uncommon and have been ascribed specific associations (*3HgOc* and

254 *4MgOc*, respectively). These associations show that the lower parts of the intermediate

255 landscape have been only very weakly eroded by the High and Middle glacia, which

256 removed the Intermediate duricrust without stripping the rest of the underlying

257 Intermediate profile. Although they correspond to glacia surfaces, these associations

258 result from weathering of the underlying bedrock.

259 Finally, similarly to the Intermediate paleolandscape, some glacia plateaus have

260 been partly eroded, leaving residual hills that are covered with scattered blocks of the

261 original duricrust. These blocks directly overly the carapace, mottled clay or saprolite

262 horizon of the weathering profile. The residual hills correspond to associations *3HgR*

and *4MgR*, for the High and Middle glacis, respectively. These associations are ambiguous as to whether they represent bedrock weathered in situ or transported material. Indeed, exhumed horizons of the weathering profile may still be fine-grained clayey to sandy detrital sediments.

3. 2. 3. *Low Glacis system (5LgD)*

A specificity of the Low glacis system is that it has remained functional in the area in the form of a regional active pediment. It is why its geomorphology and regolith shall be described in detail in section 3.4. It is however worth mentioning here that upslope portions of the Low glacis are in many locations connected to lower portions of the Middle glacis to form a single surface as a result of polygenic evolution (e.g., Figs. 4 and 5). Also, along portions of some streams, the sedimentary cover of the glacis is locally removed so that the roof of the Low glacis Fe duricrust (*5LgD*) is exposed. The map areal extent of that association is therefore very limited. But it may underlay the sedimentary blanket of the active pediment over significant areas, at least along major drains. The Low glacis Fe duricrust is detrital and mostly conglomeratic, generally thin (<0.5 m) and weakly cemented compared to that of the Middle glacis. More generally in West Africa, the Low glacis may be best capped by a carapace or may not even be indurated at all (Grandin, 1976).

3. 3. ***Erosional reliefs (Br, Sa, Wp, LtS)***

A considerable portion of the reliefs is not protected by a duricrust and is currently undergoing erosion. That erosion contributes to further exhumed bedrock and

weathering profile material that constitute detrital sediments feeding the active pediment. Erosional terrains group 4 landform-regolith associations.

The first association (*Br*, for Bedrock Slope) refers to hilly bedrock terrains that can reach 100 m in height (Fig. 13a). They form massifs elongate in the direction of the dominant NE structural grain of the rocks, with the structural fabric (schistosity) locally expressed as aligned ridges in the high-resolution topography. Massifs of volcanosediments are generally flat-topped, as opposed to hilly for metabasites. Crests of the massifs can bear scattered blocks of Bauxitic or Intermediate duricrust and very rarely remnants of saprolite. Some slopes of the massifs are incised by ravines and gullies partially filled up with bedrock and duricrust clasts.

Association *Sa* designates all the erosional terrains exposing a saprolite. By definition, saprolite derives from weathering of the bedrock. It is very fined-grained (clay-silt granulometry), pulverulent, and kaolinite rich. The saprolite is generally dark-yellowish to reddish on mafic rocks, often with whitish spots as ghosts of plagioclase crystals. On volcanosediments, it ranges in color from whitish to intense yellow. The saprolite commonly preserves ghosts of the schistosity planes and may enclose oriented platy relics of early ferruginized bedrock.

Steep slopes and talus of duricrust-capped plateaus constitute a specific landform-regolith association (*WpS* for Weathering Profile Slope). These slopes have exhumed various layers of weathering profiles (saprolite, mottled clay, carapace) that are often covered by screes of duricrust (Figs. 13b to 13d). The slopes are vegetated to various degrees as stream reappearances are common under the duricrust at the edge of plateaus. Badlands are common in these terrains (Figs. 13d), providing direct access to the weathering profile in incisions. Importantly, these terrains provide the only

access to weathering profiles underneath detrital Fe duricrusts of the High and Middle glacia.

The last association of erosional terrains is that of lithosoils (*LtS*). It consists of hilly terrains with in a thin (<50 cm) unconsolidated layer resting atop the bedrock. This layer derives from the disaggregation of the bedrock and is mostly made of the underlying bedrock clasts, ranging in size from silt to gravel (Figs. 13e and 13f). This association generally occupies smooth reliefs at the foot of the main topographic massifs and above the active pediment (Fig.4). These terrains are generally grass-covered and therefore provide less sediment to the active pediment than the other erosional terrains. Lithosoils are dark-grey on mafic rocks and propitious for agriculture. They are generally lightly ochre on volcanosediments (Figs. 13e and 13f).

3. 4. Active pediment (*ApS*, *ApT*, *ApF*)

The active pediment occupies the largest area. It is a regional surface made of quasi-planar facets connecting the foot of all reliefs to the current main river drains over distances commonly exceeding 10 km (outside the map area of Fig. 4). Its uppermost slopes do not exceed 3 % and its mean slopes are less than 1 %. Over an overwhelming part of its surface, the pediment is covered by a detrital sedimentary layer (association *ApS*, Fig. 14a), which tends to thicken downslope (generally up to several meters in thickness, except near the main river drains where channels more than 10-m deep can be filled-up by sediments). The sedimentary layer – at least its uppermost surface – is reworked at each rainy season and may therefore be considered as transiting on the pediment. Coarse material exposed at the surface of the pediment mostly consists of debris of Al-Fe and Fe duricrust, Fe nodules (Fig. 14b) and vein quartz (more rarely

bedrock), large pebbles being restricted to uppermost slopes near reliefs. There, conglomerates can locally be weakly cemented by Fe oxyhydroxides (Fig. 14c). Downslope, the pediment surface has two main lithologies: a light-colored mix of clay, silt and sand, deriving from weathering profiles (Fig. 14a) or a pellicular ferruginous gravel resting on that same light-colored material (Fig. 14b). Sections exposed in stream cuts show that alluvial gravel layer(s) underlay the fine-grained material (Figs. 14d and 14e), bearing in mind that the Low glacia detrital Fe duricrust may floor the sedimentary cover over significant areas. Weathering of the sedimentary cover is attested at depth by the development of smectite (greenish staining, Figs. 14d and 14e) or carbonate nodulation (white spots). Importantly, the fine-grained sedimentary cover of the active pediment should not be mistaken for a saprolite preserved on its bedrock.

At various locations on the active pediment, stream channels are filled-up along some of their portions by sediments (mostly fine-grained), forming alluvial terraces that may not maintain for more than a few rainy seasons. Although an integral part of the active pediment surface, these sedimentary infillings are distinct and ascribed a specific landform-regolith association (*ApT* for Active pediment Terrace).

Several alluvial fans fed by the badlands on sides of the reliefs have been mapped and are attributed to a landform-regolith association (*ApF*). These fans constitute transient piedmont accumulations of mostly fine-grained sediments (essentially reworked saprolite) and duricrust pebbles that will ultimately make their way on the active pediment surface. The fans can locally reach 10 m in thickness. They are often exploited for placer gold.

4. Terrain classification, implications for mineral exploration

4. 1. Lateritic residuum with potential supergene enrichment

That category of regolith comprises the associations related to the upper paleolandsurfaces and the upper part of their weathering profile preserved by the paleo-glacis (blue on Fig. 15). These associations expose the carapace horizon (*2InC*, *2InR*, *3HgOc*, *4MgOc*) or the duricrust (*1BxD*, *2InD*) topping a thick weathering profile resulting from protracted (>20 My) periods of intense weathering (Valeton, 1991; Beauvais and Chardon, 2013). They may therefore host anomalies forming typical mushroom-shaped halos rooted in the bedrock (e.g., Freyssinet et al., 2005; Fig. 16b). These terrains are therefore suitable for geochemical sampling. However, elements known to be mobile in supergene environments such as As, Ag, Zn, Cu, Ni, Co or U (e.g., Tardy, 1997) would be preferentially leached in the residuum (mottled clay, carapace and duricrust) of the weathering profile (these elements could still be anomalous at low concentrations, possibly reflecting an underlying mineralization). Conversely, the residuum is more likely to concentrate non-mobile metals (e.g., Al, Zr, Ti, Sb, W) than the underlying saprolite because it has undergone volume loss and because these elements are typically hosted by minerals such as quartz, zircon, rutile or anatase that can survive most intense weathering (e.g., Valeton, 1994; Freyssinet et al., 2005; Salama et al., 2020).

Weathering profiles of the upper paleolandsurfaces are known for their supergene mineral deposits in Al, Fe and Mn (e.g., Grandin, 1976; Valeton, 1994). Upper paleolandsurface remnants are preserved mostly on greenstone belts and dolerite sills, which host most known primary bedrock concentrations in West Africa (e.g., Au, Zn, Pb, Cu, Ni; Milési et al., 1992). The potential for supergene concentration in these weathering profiles is therefore high, but still largely unexplored. Of particular interest

are metals such as Ti, Zr, V, Nb, Cr, Sn, W, Th, Hf and rare earth elements (Boulangé, 1984; Braun et al., 1993; Tardy, 1997; Butt et al., 2000; Sidibé and Yalcin, 2019) that would be pre-concentrated in the bedrock.

4. 2. In-situ regolith and bedrock

This category groups erosional terrains (*Br, Sa, Wp, LtS*; Figs. 15) etched down to the bedrock or covered with unconsolidated regolith that is connected to the geological substrate from which it derives (green on Fig. 15). They are mostly restricted to the slopes and interfluves of the main topographic massifs. They are suitable for geochemical sampling because they should express anomalies connected with the bedrock. Identification and mapping of these terrains become crucial away from the main topographic massifs because they represent the only access to in-situ regolith in the low land. In these low land contexts, they are found only on the sides of paleo-glacis relict plateaus (*Sa, WtS*; Figs. 4 and 15). Low-lying composite paleo-pediment landscapes being the norm rather than the exception in West Africa (Chardon et al., 2018), particular attention should be given to this landform-regolith category. Dispersion halos are generally narrow or nearly absent in the saprolite or the bedrock (Freyssinet et al., 2005; Bamba, 2009; Anand and Butt, 2010; See Fig; 16), which form an overwhelming part of these landform-regolith associations. This therefore requires a dense sampling grid - typically 50 m - to make sure a mineralization is not missed.

4. 3. Transported regolith

4. 3. 1. Exploration challenges

This category comprises the detrital Fe duricrusts of the paleo-glacis (*3HgD*, *4MgD*) and the sedimentary cover of the active pediment (*ApS*, *ApF*, *ApT*). That domain represents by far the widest and most continuous of the study area (Red on Fig. 15). It is also the case over most of Central and Northern Burkina Faso and more generally over the northern Soudanian zone and the Sahelian zone (Fig. 2). This category of regolith masks the weathering profile and the bedrock. This means that mineral deposits may be hidden under these covers (Fig. 16a). Mineralized material can be transported on the pediment or the paleo-glacis, part of that material being trapped in the pediment sedimentary cover (loose or duricrusted) to form a “transported” anomaly (e.g., Fig. 16d and 16e). Upward gaseous transfers and insect or plant root activity can bring mineralized material to the surface of the sedimentary cover (Anand et al., 2016; Salama et al., 2016). But the expression of an anomalous halo rooted in the bedrock through a duricrusted pediment sedimentary cover, although possible, is unlikely.

Transported regolith can host secondary metal concentration such as alluvial placers, as exemplified by gold on active pediments in Burkina Faso (Ouangrawa et al., 2000; Bamba, 2010). Paleo placers should be considered in the detrital Fe duricrust of the paleo-glacis (*3HgD*, *4MgD*). Besides, gold and base metal deposits have been discovered in detrital duricrusts in other lateritic environments (Anand et al., 2019; Salama et al., 2019). Solute transport of metals (e.g. Cu, Mg, U, Ni, Au, REE; Boulangé and Colin, 1994; Sillitoe, 2005; Reich and Vasconcelos, 2015; Xueqiu et al., 2016) down the slope of pediments can also lead to exotic deposits, mostly in pediment sedimentary cover. These deposits would produce dispersion halos comparable to those formed by mechanical transport on pediments (e.g., Fig. 16d and 16e).

4. 3. 2. *Sampling strategy*

Classical soil sampling at 40-50 cm depth would most likely not attain the in-situ regolith, as the transported cover is systematically thicker. By definition, paleo-glacis duricrusts, which are all detrital, are not suitable for aiming at the regolith sitting on its parental bedrock. Sampling leaves or the bark of deeply rooted trees such as Acacia or Eucalyptus or termite mounds would be recommended (e.g., Gleeson and Poulin, 1989; Anand et al., 2014; Salama et al., 2016; Arhin et al., 2018). But systematic sampling by aircore or auger is the most appropriate to attain the saprolite underlying the transported cover. In doing so, the orientation and spacing out of the boreholes should be adapted to the potential width of the prospected mineralized bodies as the dispersion halo may be narrow or even absent in the saprolite (Fig.16). Typically, narrow (<20 m) Au-bearing quartz dikes or REE-mineralized pegmatite dikes would easily be missed if samples are more than 100 m apart. In such a case a 50-m spacing would be required. Aircore or auger sampling of the saprolite requires rigorous description of the material drilled before reaching the saprolite, as well as diagnostic identification criteria of the saprolite itself (heterogeneity, texture, occurrence of pedorelics, lithorelics, lithostructures or relict minerals, see description of association *Sa*, section 3.3). These tests should help prevent mistaking the saprolite seating on its parental bedrock for fine-grained transported material. Once the in-situ character of the regolith is attested, one should favor sampling of residuum material instead of saprolite (see section 4.1).

4. 3. 3. *Mechanical dispersion on glacis / pediment and "transported" anomalies*

Paleo-glacis relics and active pediments are not necessarily obstacles to exploration. They can also keep tracks of a mineralization exhumed in their upslope geomorphic

environment. Indeed, glacis / pediments are erosional and transportation slopes. Their detrital overburden therefore can bear erosional products of mineralized bodies and even placers (Fig. 16). Mechanical dispersion of these products on glacis / pediments should produce very wide halo stretched down slope, over hundreds of meters to several kilometers (Sanfo et al., 1993; Parisot et al., 1995; Ouangrawa et al., 1996, 2000; Bamba, 2009, 2010). Identification of such anomalies on the active pediment may be used to track its primary (endogenous) source upslope thanks to a topographic map at the appropriate resolution. The same approach may be used on paleo-glacis systems, providing the landscape at the time the considered glacis was functional is reconstituted(Chardon et al., 2018).

4. 4. Other regolith

The last category groups Paleo-glacis relicts exposing their carapace layer (*3HgC*, *4MgC*) and the residual hills of paleo-glacis systems (*3HgR*, *4MgR*) that also generally expose the carapace (orange on Fig. 15). That category has the smallest areal extent. In this category, determination of the in-situ or transported character of the regolith is not straightforward. Indeed, a glacis carapace formed by the weathering of a fine-grained transported cover may not be distinguished from one that evolved from saprolite resting on its parental bedrock. Caution is therefore required in sampling and interpreting surface geochemical results, as such material can display an anomaly rooted in the bedrock, a transported anomaly or can mask a bedrock anomaly. Only auger or aircore drilling of the deep regolith proved to seat on its bedrock can avoid errors in interpreting the geochemistry. The same care should apply to the description

of the drilled material down to the bedrock as in the case of the transported regolith (section 4.3.2).

5. Exploring for the lateral extension of an existing ore body

The prospectivity map (Fig. 15) may be used to look for the suspected continuity of a steep planar ore body. In the present case, the NE trend of steeply dipping mineralized structures is outlined by the pattern of artisanal pits aligned on the structures (Fig. 15).

The pits are restricted to the green domain (in situ regolith and bedrock; Fig. 15), as access to the mineralization is facilitated there by the absence of duricrust and partial or complete ablation of the in-situ regolith. Linear extrapolation of the mineralized trends will allow identifying the categories of regolith susceptible to overly a lateral extension of the mineralization. Given the expected behavior of a deeply rooted anomaly upward through each category of regolith (Fig. 16), one can check whether a lateral extension of the mineralization is expressed in the regolith. Outside the green domain (in situ regolith and bedrock; Fig. 15), an extension would typically not be noticed by surface sampling in the red domain (transported regolith) and potentially the orange domain (other regolith) (Fig. 15). In the green domain, soil sampling on the extrapolated structural trend would be sufficient. In the red and orange domains, trenches across the extrapolated trend, auger drilling or inclined aircore drilling would be needed to attain the regolith preserved on its parental bedrock. That approach should be complemented by sampling of the weathering profile exposed on the talus of paleo-glacis relict plateaus (*Wp*; Fig. 4, green in Fig. 15) along the extrapolated trace of the mineralization. Finally, the potential intersection of a mineralized trend with a blue domain (lateritic residuum; Fig. 15) would lead to suspect an enrichment in the

residuum in that domain if the considered element is non-mobile in the supergene environment.

6. Concluding remarks

In this paper we have proposed a landform-regolith mapping protocol adapted to the West African morphoclimatic context. That protocol particularly takes into account the detrital nature of the Fe duricrusts capping the ubiquitous relics of the paleo-pediment systems and considers the detrital sediments covering the functional pediment that may be mistaken for weathering material preserved in-situ. The landform-regolith mapping chart is declined into a prospectivity chart, which is used to recommend adapted exploration strategies. The mapping protocol further allows for the definition of exploration guides for supergene mineral concentrations.

The mapping chart is pertinent for greenstone terrains of the Soudanian and Sahelian morphoclimatic zones (typically savanna environment and drier; Fig. 1). It can also be applied to the vast low-relief areas of composite paleo-glacis landscapes lacking relics of the upper paleo land surfaces, which encompasses the various geological substrates of the sub region. In wetter (southern) West Africa (Guinean and Forest zones, Fig. 1), the Low glacis did not develop. Field reconnaissance indicates that away from topographic massifs having kept tracks of the upper paleo land surfaces, the Middle glacis is rarely duricrusted. It is capped by a carapace or, more commonly, it is not weathered beyond the mottled clay stage. In these terrains, a careful study of landforms and associated regolith should lead to the recognition / use of the associations defined in the present work.

The ubiquity of paleo- and active lateritic pediments in West Africa where Fe duricrusts had all long been considered as residual by exploration geologists urges reevaluation of landform-regolith mapping practices, dispersion models and exploration strategies. The mapping protocol developed for the West African context may prove useful elsewhere on the African continent and more generally on other tropical shields of the world. If, as in West Africa, lateritic pediments may have been overlooked in other shield terrains of the world, the renewal of the methods to access bedrock resources would be required, because they may still be underestimated.

Acknowledgments

This work was supported by the IRD (JEAi FasoLith). The contour map was provided by NordGold. We thank John Learn and particularly Claire Floriet for making this work and its publication possible. The two referees are thanked for their helpful comments.

537 **References**

- 538 Anand, R.R., Butt, C.R.M., 2010. A guide for mineral exploration through the regolith in
539 the Yilgarn Craton, Western Australia. *Aust. J. Earth Sci.* 57, 1015–1114.
- 540 Anand, R.R., Churchward, H.M., Smith, R.E., Smith, K., Gozzard, J.R., Craig, M., Munday,
541 T.J., 1993. Classification and atlas of regolith-landform mapping units:
542 Exploration perspectives for the Yilgarn Craton. CSIRO Division of Exploration
543 and Mining, Wembrey, Report 440R, 87p.
- 544 Anand, R., Lintern, M., Noble, R., Aspandiar, M., Macfarlane, C., Hough, R., Stewart, A.,
545 Wakelin, S., Townley, B., Reid, N., 2014. Geochemical dispersion through
546 transported cover in regolith-dominated terrains—toward an understanding of
547 process. *Soc. Econ. Geol. Spec. Publ.* 18, 97–125.
- 548 Anand, R.R., Aspandiar, M.F., Noble, R.R.P., 2016. A review of metal transfer mechanisms
549 through transported cover with emphasis on the vadose zone within the
550 Australian regolith. *Ore Geol. Rev.* 73, 394–416.
- 551 Anand, R.R., Hough, R.M., Salama, W., Aspandiar, M.F., Butt, C.R.M., González-Álvarez, I.,
552 Metelka, V., 2019. Gold and pathfinder elements in ferricrete gold deposits of
553 the Yilgarn Craton of Western Australia: A review with new concepts. *Ore Geol.*
554 *Rev.* 104, 294–355.
- 555 Arhin, E., Jenkin, G.R.T., Cunningham, D., Nude, P., 2015. Regolith mapping of deeply
556 weathered terrain in savannah regions of the Birimian Lawra Greenstone Belt,
557 Ghana. *J. Geochem. Explor.* 159, 194–207.
- 558 Arhin, E., Torkornoo, S., Zango, M.S., Kazapoe, R., 2018. Gold in Plant: a biogeochemical
559 approach in detecting gold anomalies undercover-a case study at Pelangio Gold
560 Project at Mamfo area of BrongAhafo, Ghana. *Ghana Min. J.* 18, 39–48.

561 Bamba, O., 2010. Évolution géodynamique externe et implication sur le devenir de l'or en
562 contexte sub-sahélien. *Can. J. Earth Sci.* 47, 1–12.

563 Bamba, O., 2009. Morphopédologie et anomalie géochimique. *Can. J. Earth Sci.* 46, 939–
564 947.

565 Beauvais, A., Chardon, D., 2013. Modes, tempo, and spatial variability of Cenozoic
566 cratonic denudation: The West African example. *Geochem. Geophys. Geosyst.*
567 14, 1590–1608.

568 Beauvais, A., Ruffet, G., Hénocque, O., Colin, F., 2008. Chemical and physical erosion
569 rhythms of the West African Cenozoic morphogenesis: The ³⁹Ar–⁴⁰Ar dating of
570 supergene K-Mn oxides. *J. Geophys. Res.-Earth Surface* 113, F4007.

571 Boeglin, J.-L., Mazaltarim, D., 1989. Géochimie, degré d'évolution et lithodépendance
572 des cuirasses ferrugineuses de la région de Gaoua au Burkina Faso. *Sci. Géol.*
573 *Bull.* 42, 27–44.

574 Bolster, S.J.S., 1999. Regolith mapping: Is it really necessary? *Explor. Geochem. Aust. Inst.*
575 *Geosci. Bull.* 30, 125–135.

576 Boulangé, B., 1986. Relation between lateritic bauxitization and evolution of landscape.
577 *Trav. Int. Com. Stud. Bauxite, Alumina & Aliminum (ISCOBA)* 16–17, 27–44.

578 Boulangé, B., 1984. Les formations bauxitiques latéritiques de Côte d'Ivoire : les faciès,
579 leur transformation, leur distribution et l'évolution du modelé. *Trav. Doc.*
580 *ORSTOM* 175, 1–342.

581 Boulangé, B., Colin, F., 1994. Rare earth element mobility during conversion of nepheline
582 syenite into lateritic bauxite at Passa Quatro, Minas Gerais, Brazil. *Appl.*
583 *Geochem.* 9, 701–711.

584 Bowell, R.J., Afreh, E.O., Laffoley, N.d.'A., Hanssen, E., Abe, S., Yao, R.K., Pohl, D., 1996.
 585 Geochemical exploration for gold in tropical soils. Four contrasting case studies
 586 from West Africa. *Trans. Inst. Min. Metall. Sect. B Appl. Earth Sci.* 105, B12-B33.
 587 Braun, J.-J., Pagel, M., Herbillin, A., Rosin, C., 1993. Mobilization and redistribution of
 588 REEs and thorium in a syenitic lateritic profile: A mass balance study. *Geochim.*
 589 *Cosmochim. Acta* 57, 4419–4434.
 590 Butt, C.R.M., 2016. The development of regolith exploration geochemistry in the tropics
 591 and sub-tropics. *Ore Geol. Rev.* 73, 380–393.
 592 Butt, C.R.M., Bristow, A.P.J., 2013. Relief inversion in the geomorphological evolution of
 593 sub-Saharan West Africa. *Geomorphology* 185, 16–26.
 594 Butt, C.R.M., Lintern, M.J., Anand, R.R., 2000. Evolution of regoliths and landscapes in
 595 deeply weathered terrain—implications for geochemical exploration. *Ore Geol.*
 596 *Rev.* 16, 167–183.
 597 Castaing, C., Billa, M., Milesi, J.P., Thiéblemont, D., Le Metour, J., Égal, E., Donzeau, M.,
 598 Guerrot, C., Cocherie, A., Chèvremont, P., 2003. Carte géologique et minière du
 599 Burkina Faso à 1/1 000 000. BRGM/BUMIGEB.
 600 Chardon, D., Grimaud, J.-L., Beauvais, A., Bamba, O., 2018. West African lateritic
 601 pediments: Landform-regolith evolution processes and mineral exploration
 602 pitfalls. *Earth-Sci. Rev.* 179, 124–146.
 603 Freyssinet, P., Butt, C.R.M., Morris, R.C., Piantone, P., 2005. Ore-forming processes
 604 related to lateritic weathering. *Econ. Geol. 100th Anniversary Volume*, 681–722.
 605 Gleeson, C.F., Poulin, R., 1989. Gold exploration in Niger using soils and termitaria. *J.*
 606 *Geochem. Explor.* 31, 253–283.

607 Grandin, G., 1976. Aplaniissements cuirassés et enrichissement des gisements de
 608 manganèse dans quelques régions d'Afrique de l'Ouest. Mém. ORSTOM 82, 1–276.
 609 Grimaud, J.-L., Chardon, D., Metelka, V., Beauvais, A., Bamba, O., 2015. Neogene
 610 cratonic erosion fluxes and landform evolution processes from regional regolith
 611 mapping (Burkina Faso, West Africa). *Geomorphology* 241, 315–330.
 612 Milési, J.-P., Ledru, P., Feybesse, J.-L., Dommanget, A., Marcoux, E., 1992. Early
 613 Proterozoic ore deposits and tectonics of the Birimian orogenic belt, West Africa.
 614 *Precambrian Res.* 58, 305–344.
 615 Ouangrawa, M., Grandin, G., Parisot, J.-C., Baras, E., 1996. Dispersion mécanique de
 616 l'or dans les matériaux de surface : exemple du site aurifère de Piéla (Burkina-
 617 Faso). *Pangea* 25, 25–40.
 618 Ouangrawa, M., Grandin, G., Parisot, J.-C., Delaune, M., 2000. Evolution des
 619 particules d'or en milieu lateritique soudano-sahélien : Alluvions et
 620 colluvions dans l'environnement d'un gîte filonien, Piéla, Burkina Faso. *Bull. Soc.*
 621 *Géol. Fr.* 171, 397–405.
 622 Parisot, J.-C., Ventose, V., Grandin, G., Bourges, F., Debat, P., Tollon, F., Millo, L., 1995.
 623 Dynamique de l'or et d'autres minéraux lourds dans un profil d'altération cuirassé
 624 du Burkina Faso, Afrique de l'Ouest. Intérêt pour l'interprétation de la mise en
 625 place des matériaux constituant les cuirasses de haut glacis. *C.R. Acad. Sci. Paris*
 626 321, 295–302.
 627 Reich, M., Vasconcelos, P., 2015. Geological and economic significance of supergene
 628 metal deposits. *Elements* 11, 305–310.

629 Roquin, C., Freyssinet, P., Zeegers, H., Tardy, Y., 1990. Element distribution patterns in
630 laterites of southern Mali: consequence for geochemical prospecting and
631 mineral exploration. *Appl. Geochem.* 5, 303–315.

632 Salama, W., Anand, R., Morey, A., Williams, L., 2019. Supergene gold in silcrete as a
633 vector to the Scuddles volcanic massive sulfides, Western Australia. *Miner.*
634 *Deposita* 54, 1207–1228.

635 Salama, W., Anand, R., Roberts, M., Smith, R.E., 2020. A regolith geochemical anomaly
636 formed by accumulation and corrosion of resistant minerals from Scuddles VMS
637 primary ore, Western Australia. *J. Geochem. Explor.* 106520.

638 Salama, W., Gazley, M.F., Bonnett, L.C., 2016. Geochemical exploration for supergene
639 copper oxide deposits, Mount Isa Inlier, NW Queensland, Australia. *J. Geochem.*
640 *Explor.* 168, 72–102.

641 Sanfo, Z., Colin, F., Delaune, M., Boulangé, B., Parisot, J.-C., Bradley, R., Bratt, J., 1993.
642 Gold: a useful tracer in subsahelian laterites. *Chem. Geol.* 107, 323–326.

643 Sidibé, M., Yalcin, M., 2019. Petrography, mineralogy, geochemistry and genesis of the
644 Balaya bauxite deposits in Kindia region, Maritime Guinea, West Africa. *J. Afr.*
645 *Earth Sci.* 149, 348–366.

646 Sillitoe, R.H., 2005. Supergene oxidized and enriched porphyry copper and related
647 deposits. *Econ. Geol.* 100, 723–768.

648 Tardy, Y., 1997. Petrology of laterites and tropical soils. Balkema, Rotterdam.

649 Valeton, I., 1994. Element concentration and formation of ore deposits by weathering.
650 *Catena* 21, 99–129.

651 Valeton, I., 1991. Bauxites and associated terrestrial sediments in Nigeria and their
652 position in the bauxite belts of Africa. *J. Afr. Earth Sci.* 12, 297–310.

653 Xueqiu, W., Bimin, Z., Xin, L., Shanfa, X., Wensheng, Y., Rong, Y., 2016. Geochemical
654 challenges of diverse regolith-covered terrains for mineral exploration in China.
655 Ore Geol. Rev. 73, 417–431.

656 Zeegers, H., Lecomte, P., 1992. Seasonally humid tropical terrains (savannas), in: Butt,
657 C.R.M., Zeegers, H. (Eds.), Regolith Exploration Geochemistry in Tropical and
658 Subtropical Terrains. Elsevier, Amsterdam, pp. 203–240.

659

660

Figure captions

Figure 1. Synthetic representation of the West African morpho-climatic sequence of duricrusted lateritic paleolandsurfaces(after Chardon et al., 2018). Abandonment ages of the paleolandsurfaces are after Beauvais et al.(2008)and Beauvais and Chardon (2013).

Figure 2. Climatic zonation of West Africa with location of the study area in the southern West African craton.

Figure 3.Geology and topography of the study area with the main field stations, itineraries and the artisanal mining pits (1 m contour topography, UTM , zone 30N, WGS84).

Figure 4.Landform-regolith map and chart.The contours are 1 m. Associations 3HgOc, 4MgOc and ApT are documented in the wider study area but not on that specific map extract.

Figure 5.Synthetic cross-section showing the main landform-regolith associations in their geomorphic context. The line of section is located on the map of Figure 4. Only the geomorphological type 1 of the Intermediate paleolandsurface occurs on that cross-section.

Figure 6.Geomorphology of upper paleolandsurfaces. (a) Bauxitic plateau. The plateau is 2-km-wide and 130 m high. (b) Ridges of the Intermediate paleolandsurface 50 m under a bauxitic plateau (type 1 geomorphic occurrence). Dry grass-covered upslope portion of the active pediment in the foreground. (c) Plateaus of the Intermediate paleolandsurface (type 2 occurrences; height 60 m). The lowland consists in the active pediment.

Figure 7.Main petrographic types of duricrusts capping the bauxitic paleolandsurface (1BxD). (a)-(b) Heterogeneous breccia-like bauxite. (c) Massive bauxite. (d) Massive bauxite preserving pedorelics of pinkish saprolite. (e) Nodular Fe bauxite. (f) Pisolitic Fe bauxite (pisoliths have dark nucleus and violet cortexes). Geological substrates are volcanosediments for (a)-(c) and metabasic rocks for (d)-(f).

Figure 8.Main types of Intermediate duricrust (2InD). (a)-(d) are Al-Fe duricrusts from ridges flanking bauxitic plateaus (geomorphic type 1); (e) and (f) are Fe duricrusts typical of isolated plateaus (geomorphic type 2). (a) Dismantled duricrust. (b) Heterogeneous type with relict white / yellowish Al-Fe patches in dark-violet Fe-rich medium (mostly Fe oxyhydroxides and kaolinite). (c) Nodular to proto-pisolitic (yellowish nodules cortexes are made of clay minerals, mostly kaolinite). (d) Bauxitic duricrust relic (white) partly "digested" in an Intermediate Al-Fe duricrust (dark). (e) Concretional Fe duricrust made of coalescent nodules (dark-violet on fresh cut). (f) Dark-violet Fe duricrust with tubular voids filled with a mix of clay minerals and Fe oxyhydroxides. (e) and (f) are essentially of the same type, and may host clayey pedorelics.

Figure 9. Main types of carapace of the Intermediate weathering profile. (a) Nodular, with abundant matrix. (b) Packed nodular (i.e., with less abundant matrix). (c) Conglomerate-like, with abundant angular and sub-angular nodules and concretions. This type generally occurs right under the duricrust horizon in the weathering profile (nodule-rich layer forming the “root” of the duricrust).

Figure 10. Geomorphology of paleopediment systems. (a) High glacia forming the piedmont of a bauxitic plateau. (b) Stepped relics of the High and Middle glacia on the piedmont of a bauxitic plateau (background). (c) Composite (polygenic) glacia relic made of the High glacia (upslope) and the Middle Glacia (downslope) (maximum height of plateau: 25 m). One notes a difference in the thickness of the duricrust between the High and the Middle glacia. The break of slope between the two glacia systems is rarely detectable in the field but is visible on high-resolution topography. (d) Low-lying relics of the Middle glacia (a few meters high). The plateau relic in the foreground is capped by a Fe duricrust forming a scarplet. That in the background has become residual hills topped only the carapace layer (the duricrust has been eroded away). This corresponds to the *4MgR* association (Fig. 4).

Figure 11. Regolith types of the paleo-pediment systems. (a) Upper weathering profile of the High glacia (on volcanosedimentary substrate). S: saprolite horizon, MC: mottled clay horizon, C: Carapace horizon, D: Fe duricrust. (b) Carapace and topping duricrust of the Middle glacia. The duricrust is a cemented conglomerate made of gravel- and cobble-sized pebbles. (c) Conglomeratic Fe duricrust of the High glacia formed by debris flow. Light-colored cobbles are bauxites and dark ones are Intermediate Fe

duricrust; the matrix is made of gravel-sized Fe oxyhydroxide nodules and clasts. (d) Detrital Fe duricrust of the High glacia, typical of the lowermost portions of glacia relics. Pebbles are mostly bauxite clasts (light colored) and Fe oxyhydroxide nodules. The matrix is made of a mix of clay minerals and Fe oxyhydroxides (orange color) as well as Fe oxyhydroxide-rich patches. (e) Detrital Fe duricrust of the Middle glacia comparable to (d) except for the occurrence of vacuoles, a higher porosity and a higher quartz content. (f) Gravel-sized conglomeratic Fe duricrust of the Middle glacia with a dominant vacuole-rich clayey matrix.

Figure 12. (a) Typical sandy vacuolar carapace of the High glacia. Before exposure, voids were filled with a loose clayey mix of clay minerals and Fe oxyhydroxides. (b) High glacia carapace with preserved bedrock structure, resulting from iron impregnation in the upper saprolite.

Figure 13. Erosional terrains. (a) Hilly bedrock landscape (metabasic rocks). (b) Saprolite exposed as a result of stripping of the bauxitic paleolandscape (preserved in the background). (c) Kaolinite (saprolite) exposed in a gully along a steep slope of a bauxitic plateau (note scree blanketing the saprolite to the right). (d) Talus under the edge of a duricrust-capped High glacia plateau (height: 25 m). Ravines and gullies on the talus slope provide access to various horizons of the weathering profile underlying the duricrust. In the foreground: active pediment showing detrital material (reworked saprolite) in transit in ephemeral streams. (e)-(f) Surface aspect of lithosols on metabasic/volcanosedimentary rocks, respectively.

Figure 14. Geomorphology and regolith of the active pediment. (a) General view of the pediment surface with two main types of sedimentary cover: gravel (brown) and light-colored clayey-silty material (bauxitic plateaus in the background). (b) Detailed view of the gravel, which consists in a very thin blanket on the clayey-silty material. (c) Weakly cemented debris flow material resting directly on the saprolite horizon of a truncated weathering profile (uppermost portion of the pediment). (d)-(e) Stream cutsthrough the pediment detrital sedimentary cover. (d) Clayey-sandy layer topping a gravel layer. Greenish staining of the gravel layer indicates post-alluvial development of smectite. (e) Two gravel layers topped by clay-sandy material. The lower gravel layer has undergone slight smectitic weathering.

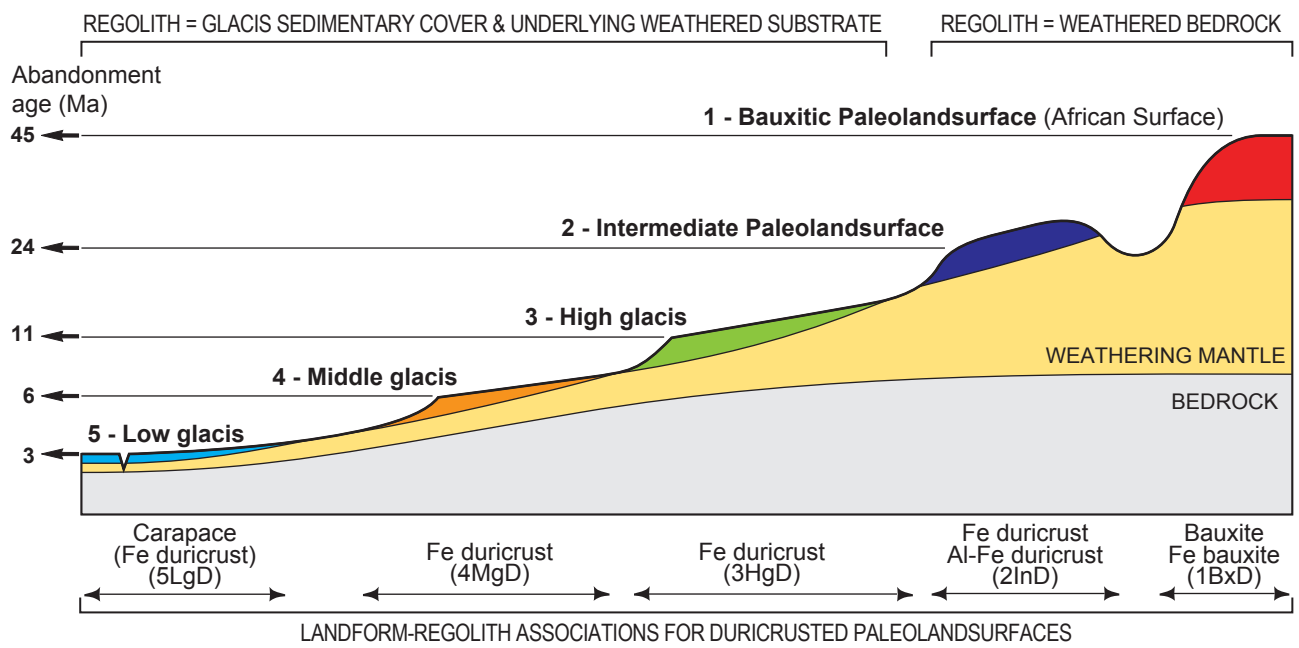
Figure 15. Soil prospectivity map deduced from the landform-regolith map of Figure 4. Compare to Figure 4 to see how each landform-regolith associations has been assigned to one of the four categories of regolith (see text for further explanation). The mineralized structural trends are based on the alignment of the artisanal mining pits.

Figure 16. Idealized geochemical dispersion halos in West African granite-greenstone terrains. In (a), the mineralization (and its potential halo) is truncated by a glacia/pediment. In (b), the mineralized structure crops out; there is no dispersion halo and therefore little chance to detect the mineralization. In (c), a mushroom-shape halo forms entering the residuum of the weathering profile and an in-situ geochemical anomaly may be detected. In (d) and (e), a dispersion halo forms by mechanical transport of mineralized material in the pediment detrital cover. Transported cover in (a) would essentially be a detrital Fe-duricrust and in (d) and (e) unconsolidated detrital

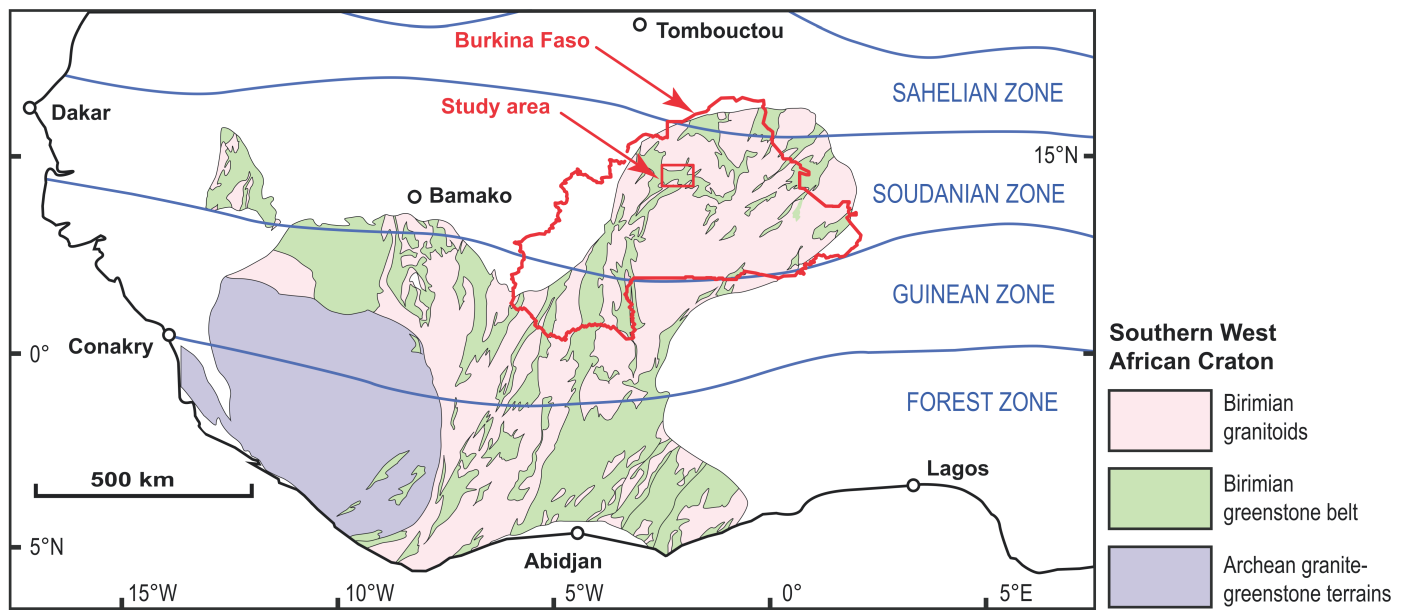
780 sediments. In (e), the halo may be detected by surface sampling, whereas in (d) it is
781 buried and therefore inaccessible. Situation (a) would typically occur under relics of the
782 High or Middle glacia, situation (c) under relics of the bauxitic and/or Intermediate
783 paleo land surfaces, whereas situations (d) and (e) would be typical of the active
784 pediment, bearing in mind that detrital Fe duricrust-capped paleo-glacia systems can
785 host (d) and (e) types of halo. These types of halo can also form by downslope element
786 transport in solution, on the pediment sedimentary cover.

787

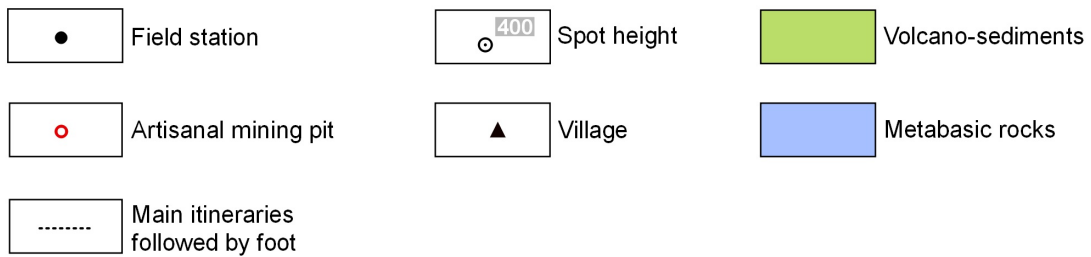
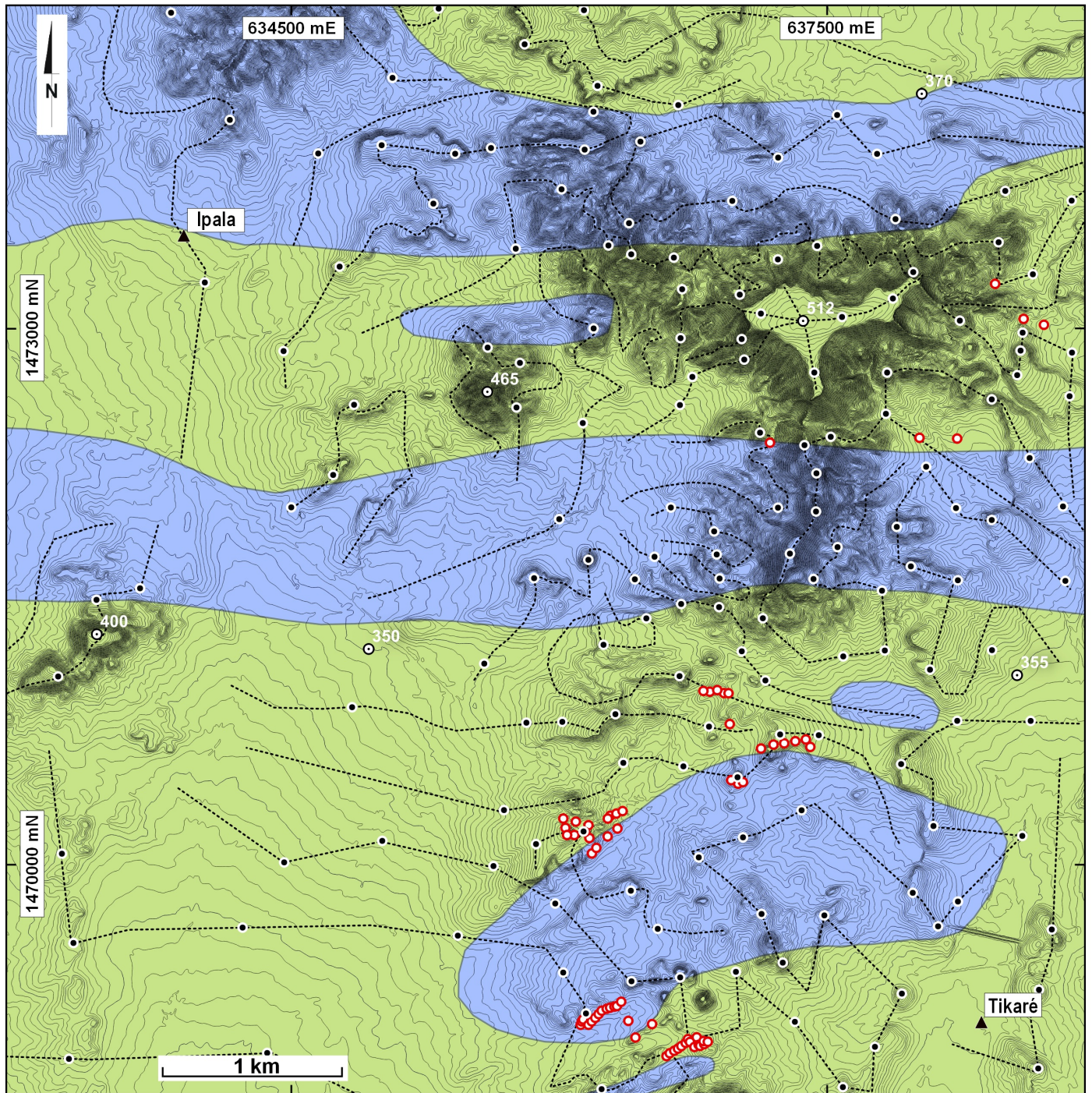
788



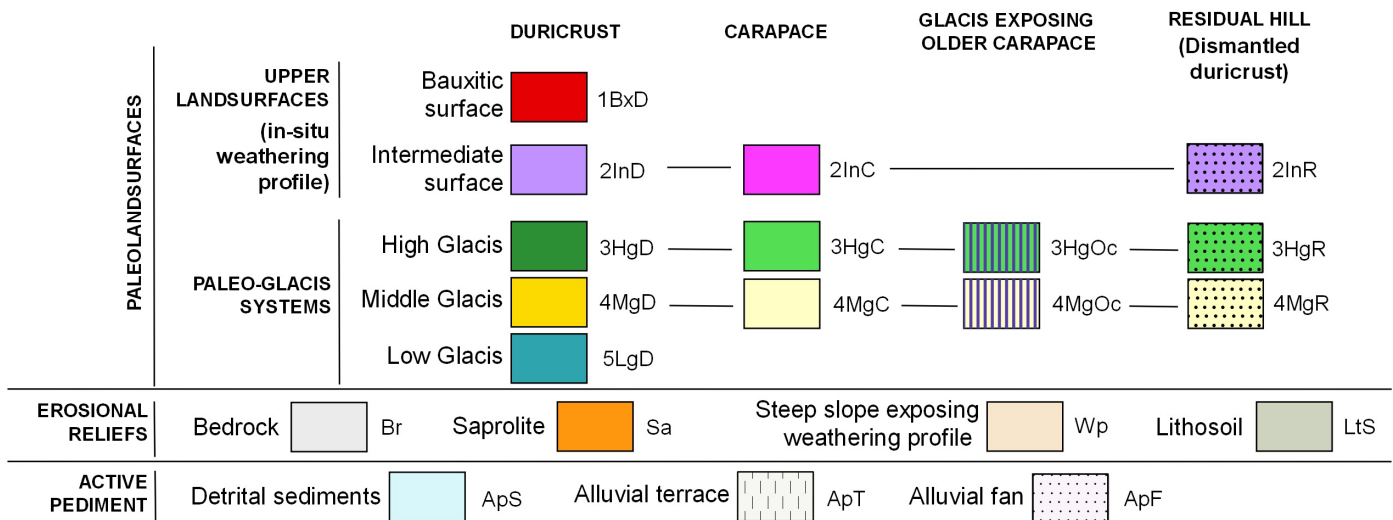
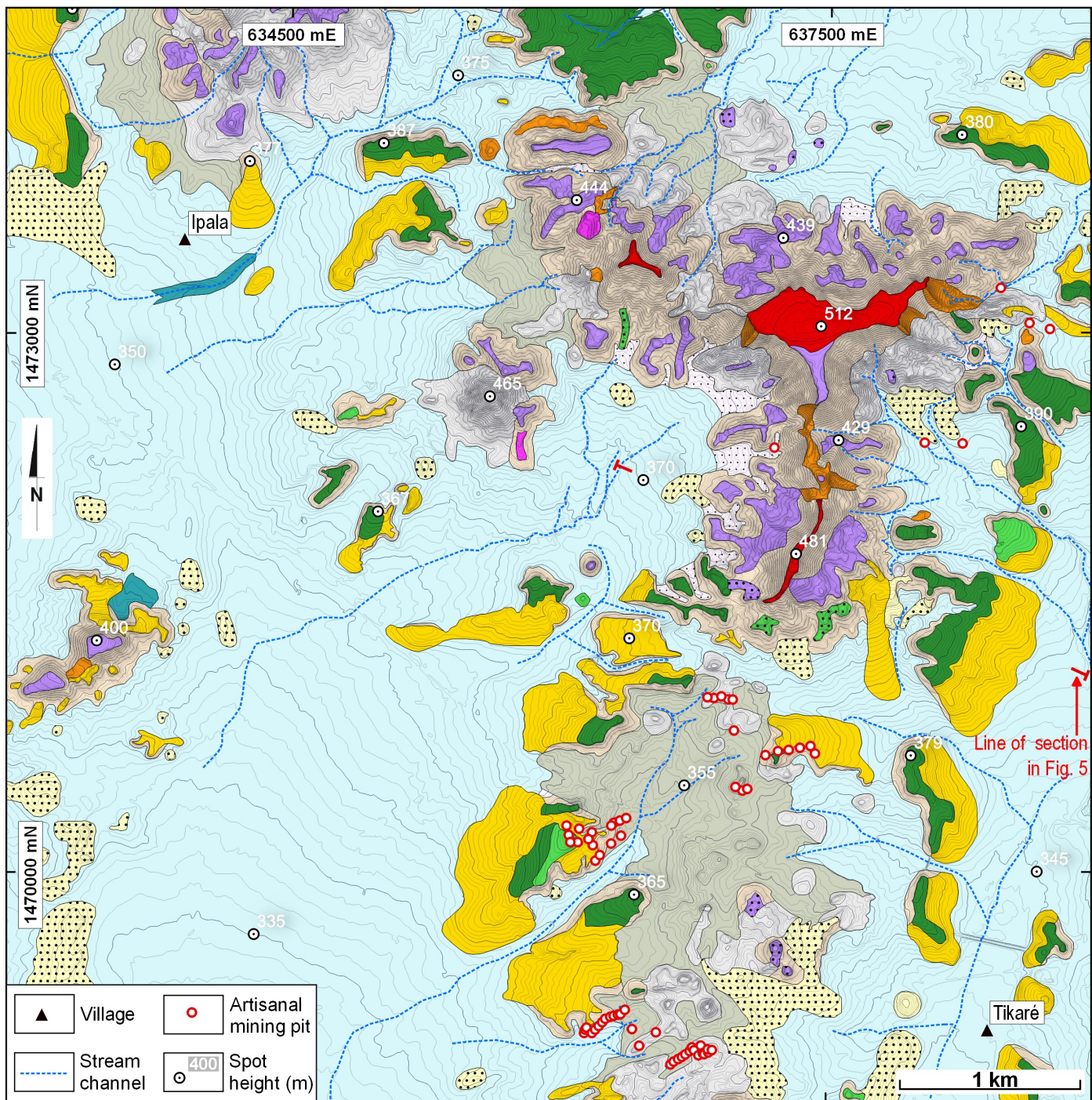
Sawadogo et al. Figure 1



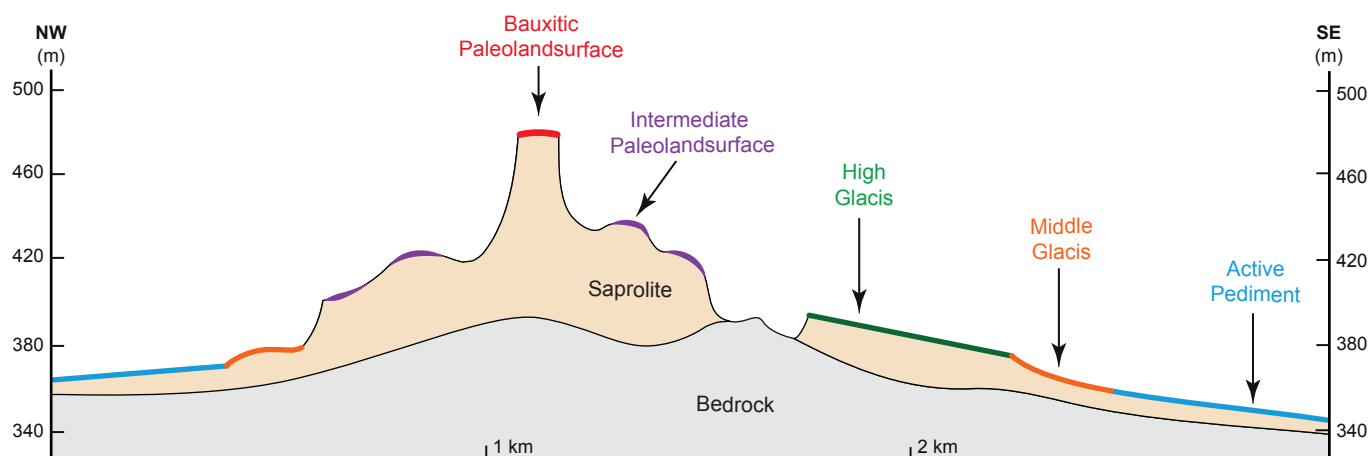
Sawadogo et al. Figure 2



Sawadogo et al. Figure 3



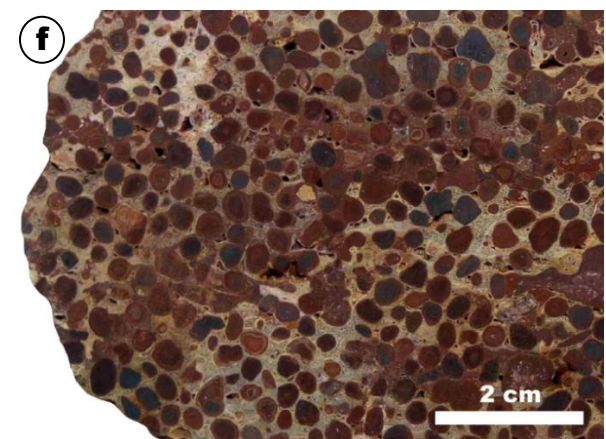
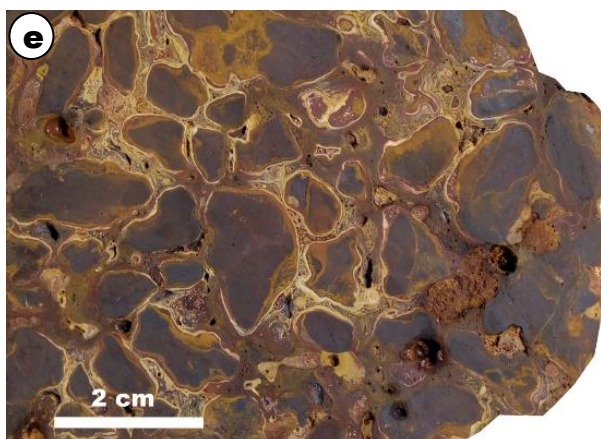
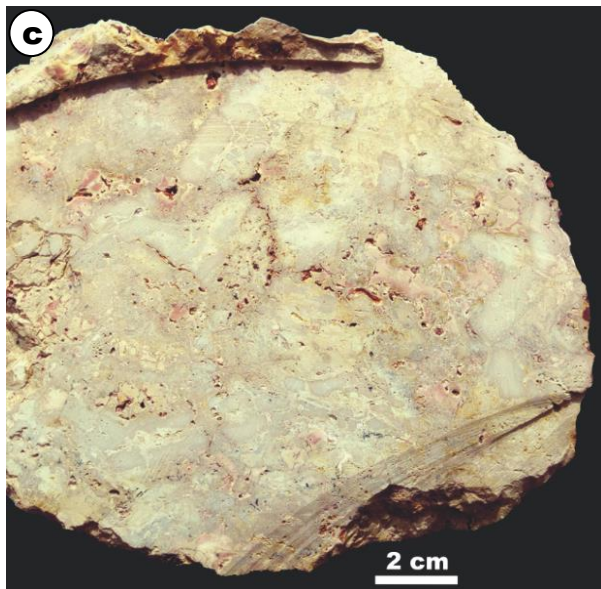
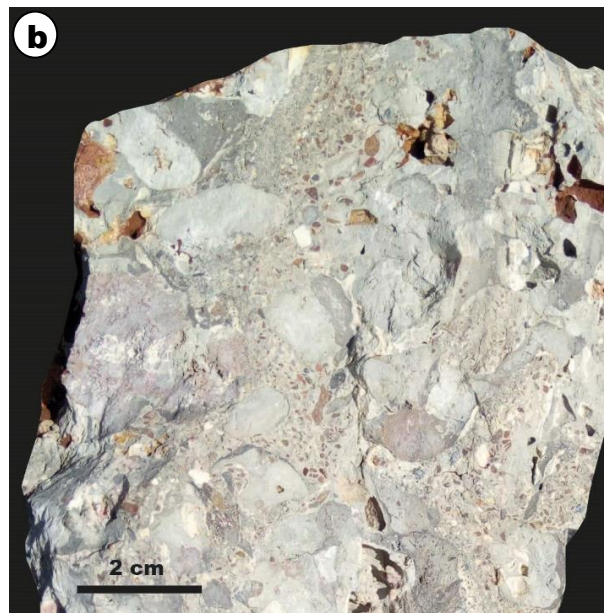
Sawadogo et al. Figure 4



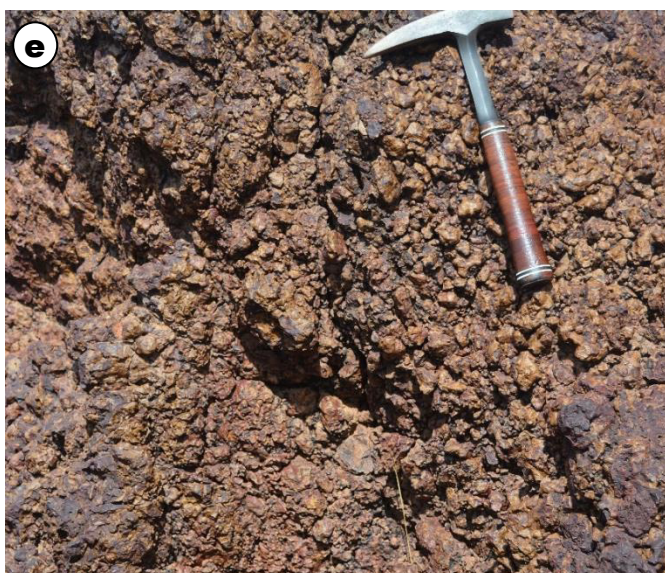
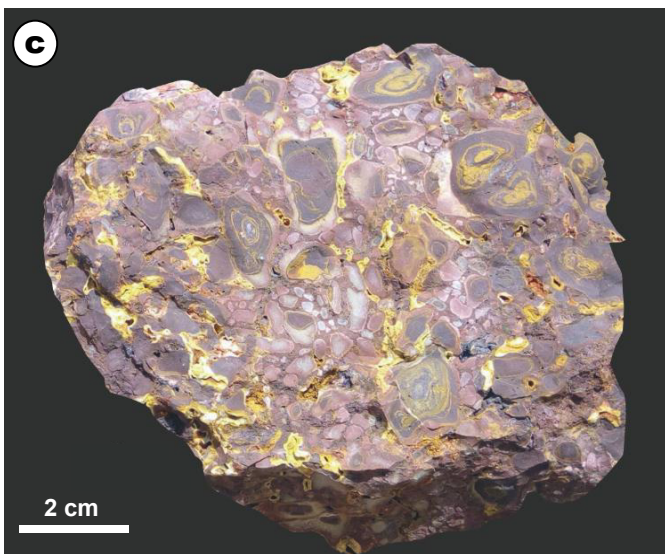
Sawadogo et al. Figure 5



Sawadogo et al. Figure 6



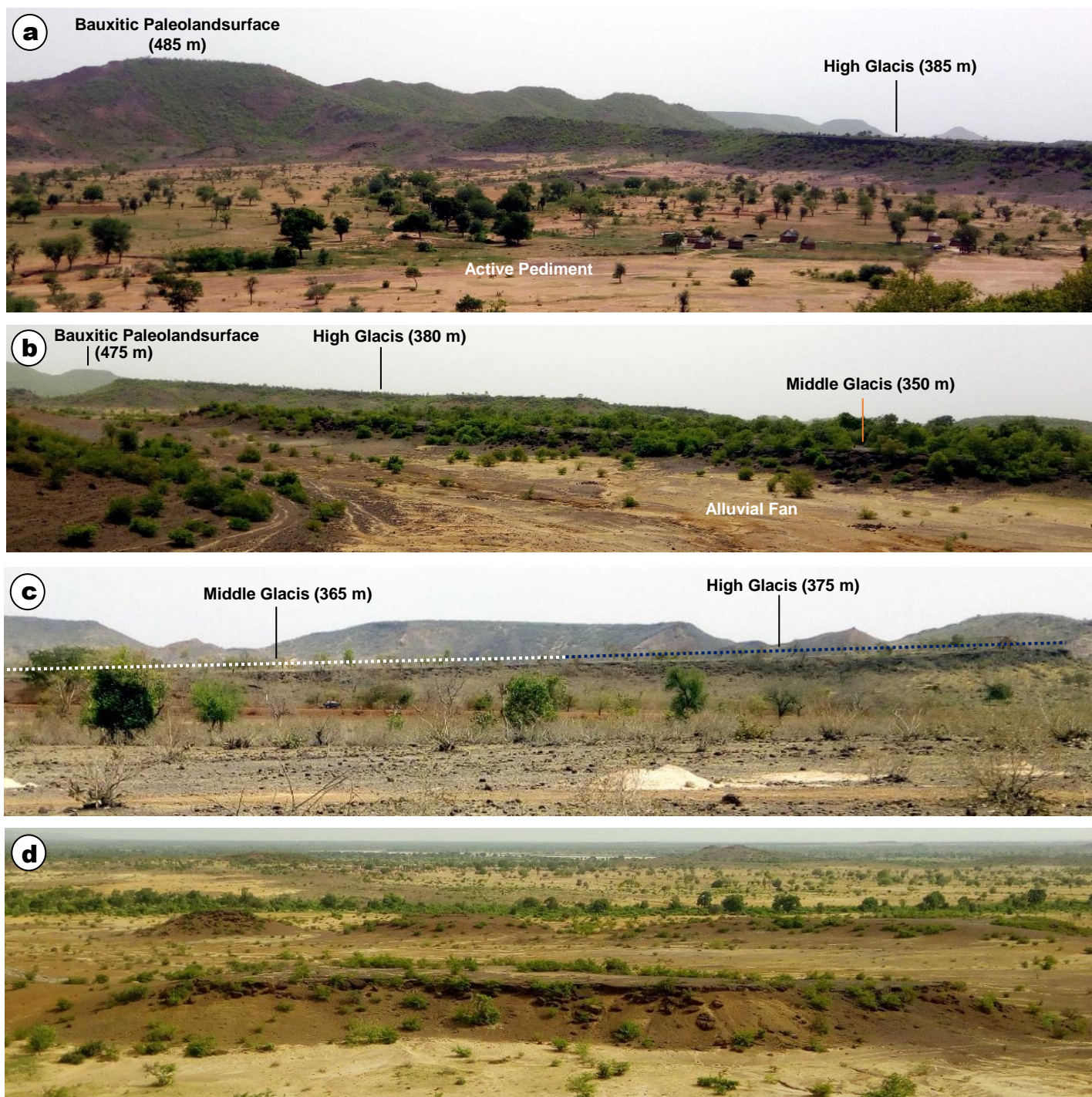
Sawadogo et al. Figure 7



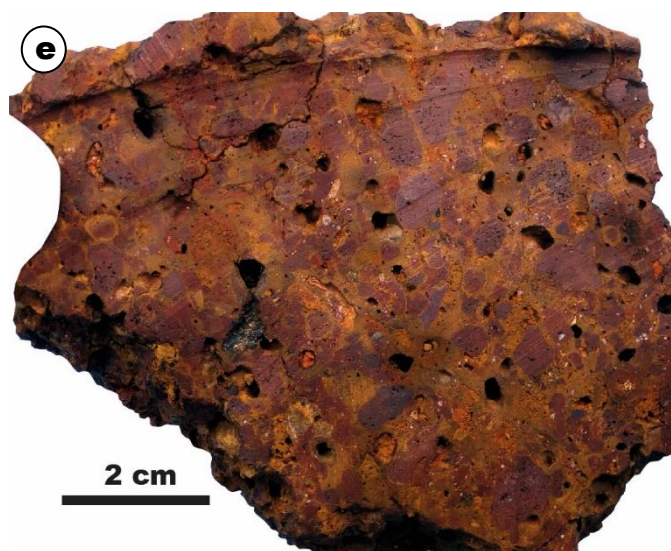
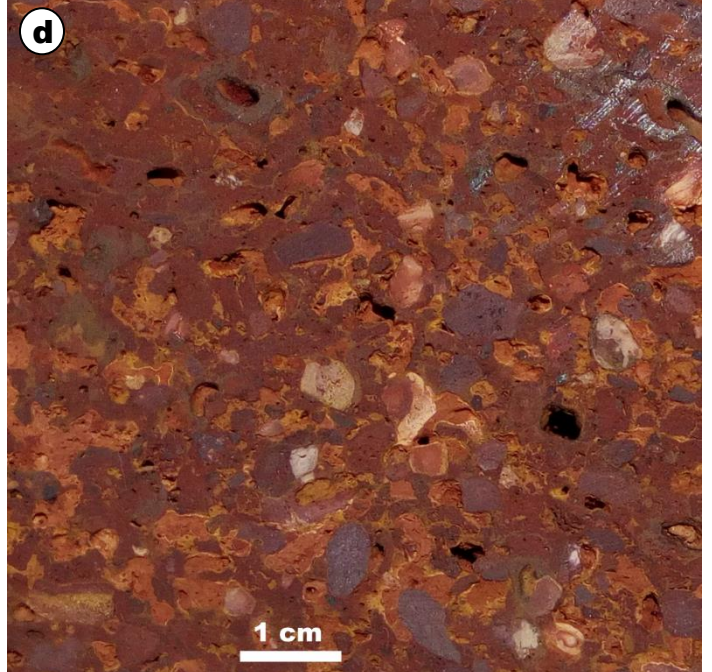
Sawadogo et al. Figure 8



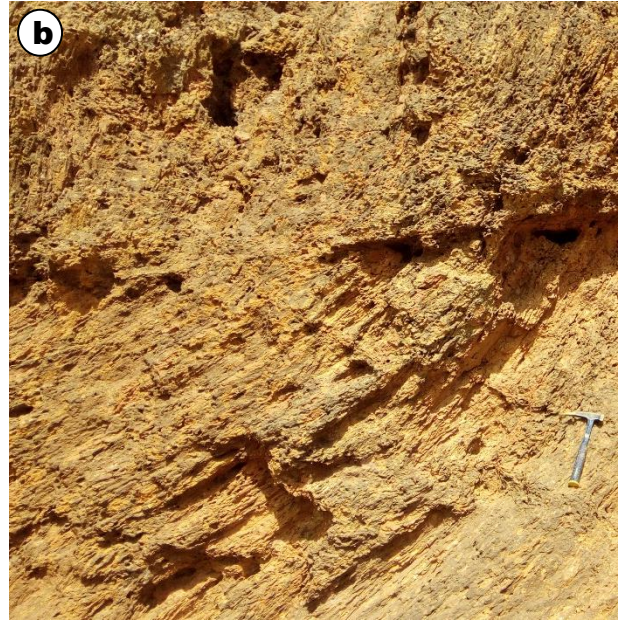
Sawadogo et al. Figure 9



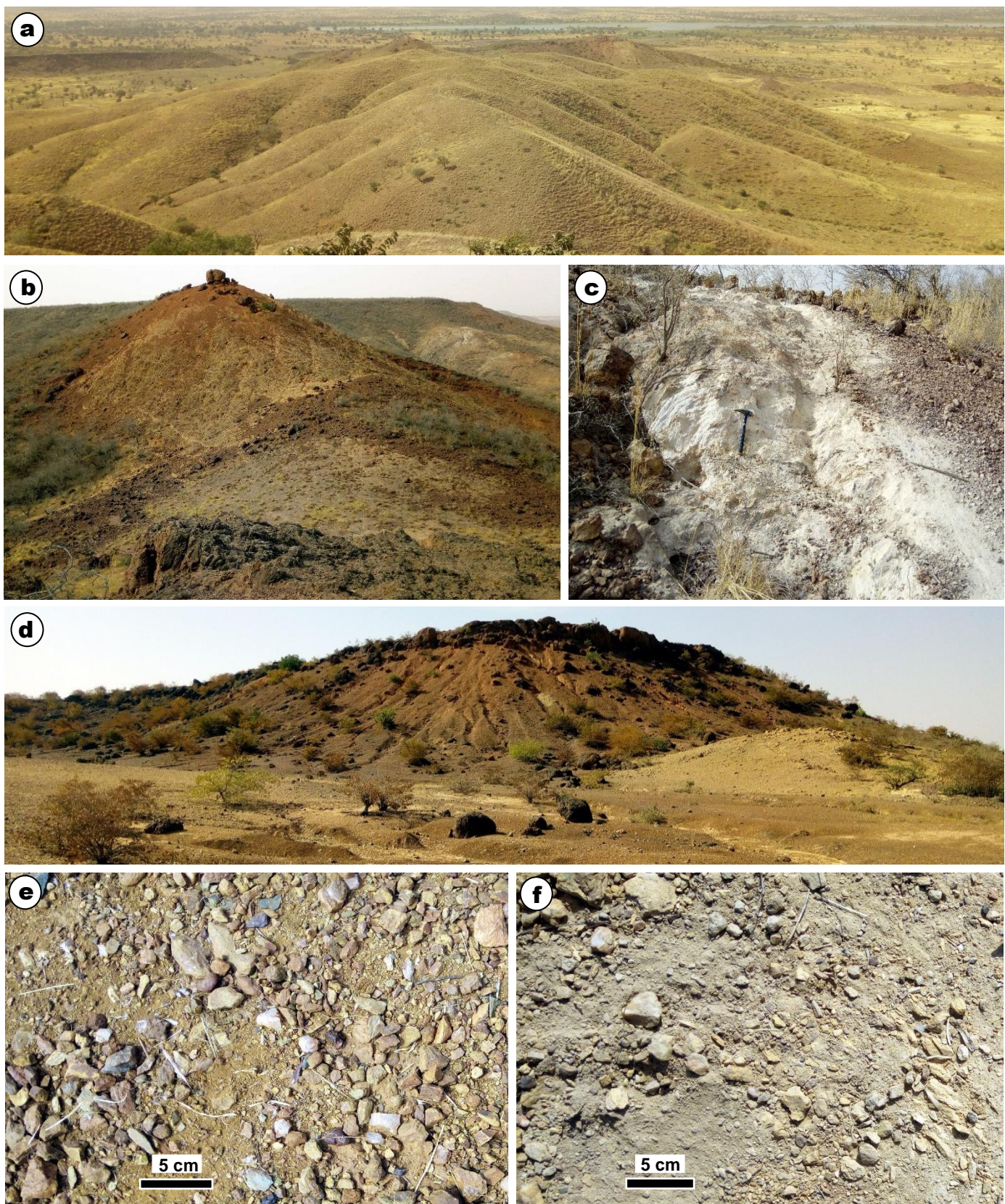
Sawadogo et al. Figure 10



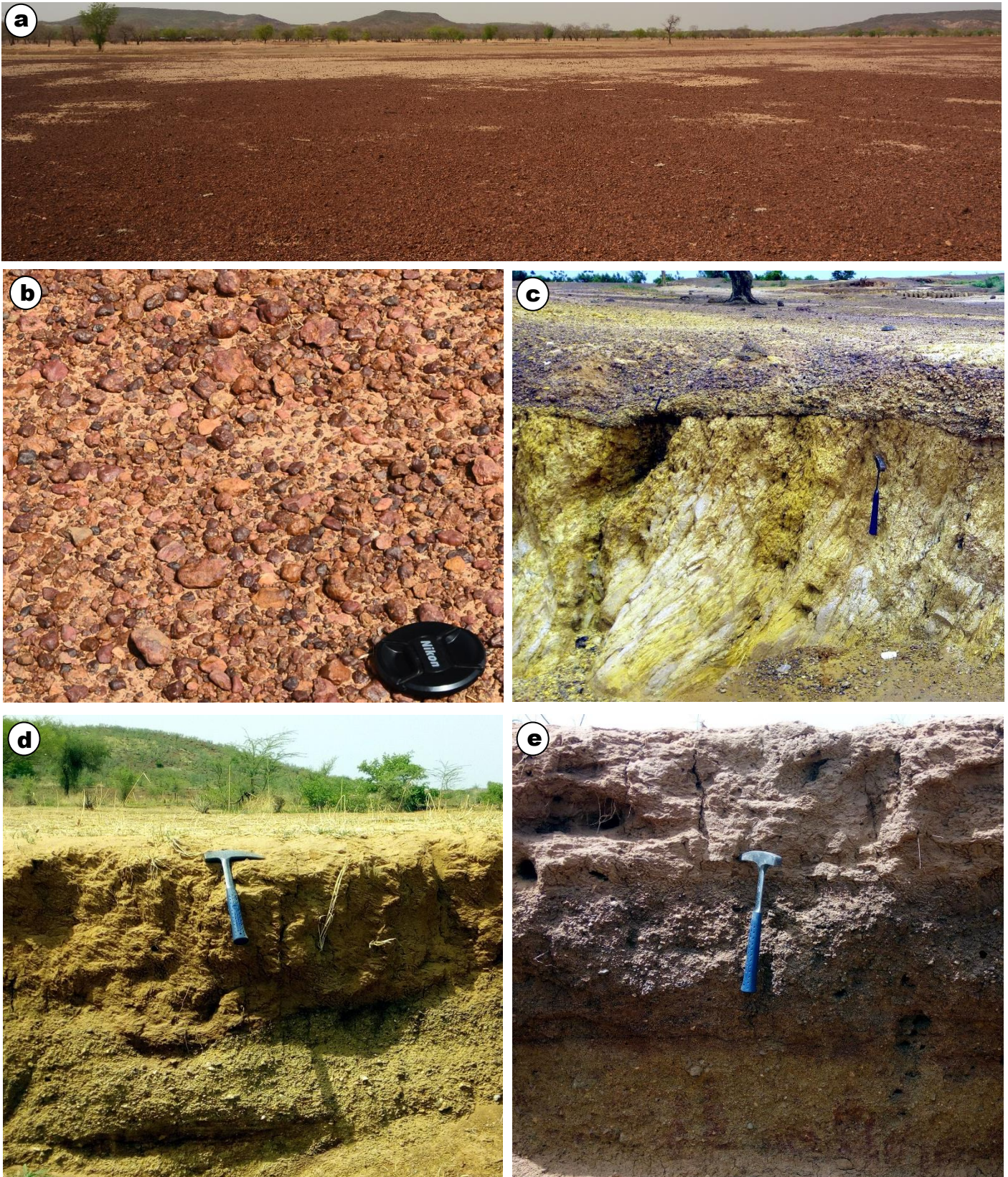
Sawadogo et al. Figure 11



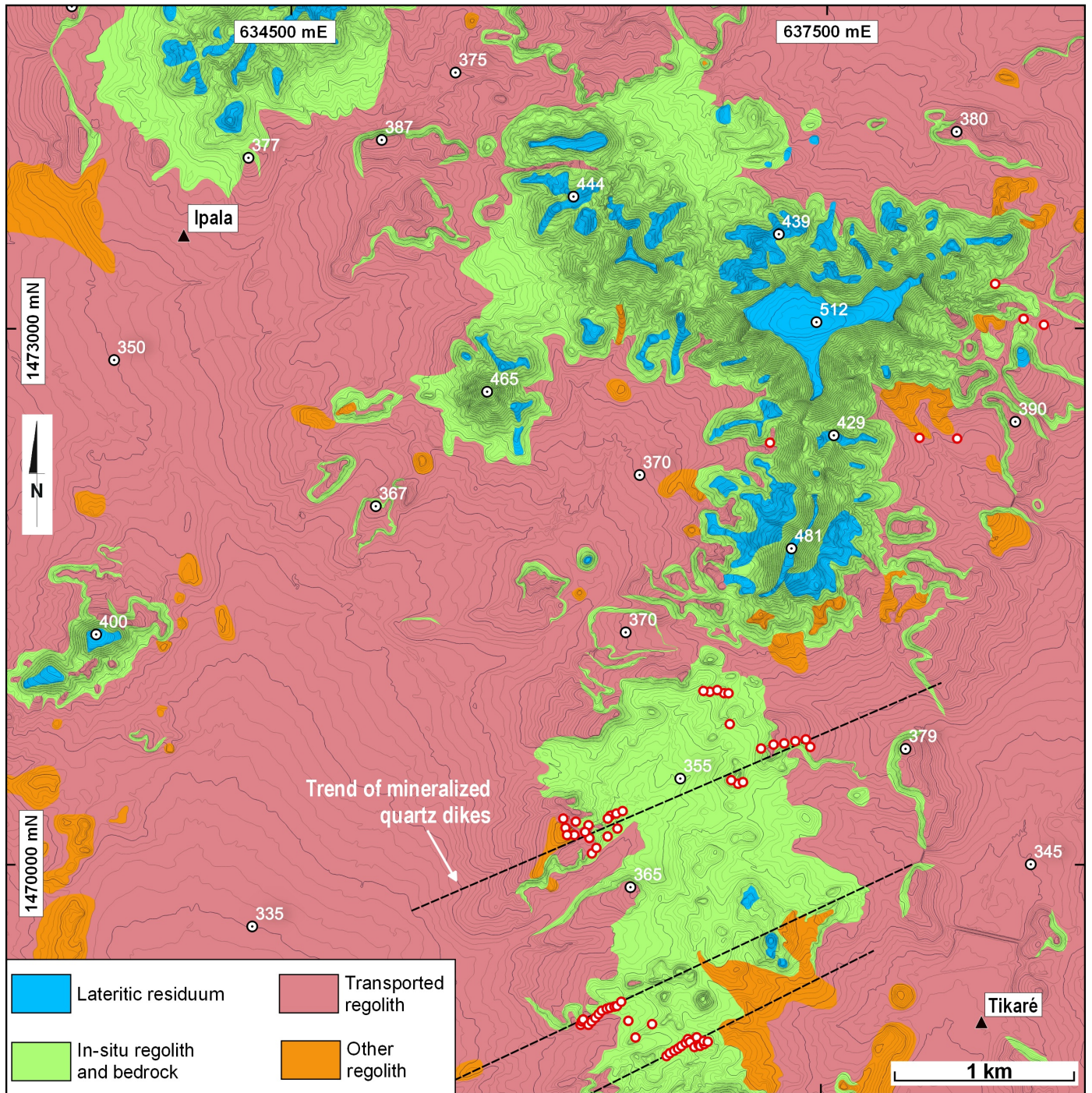
Sawadogo et al. Figure 12



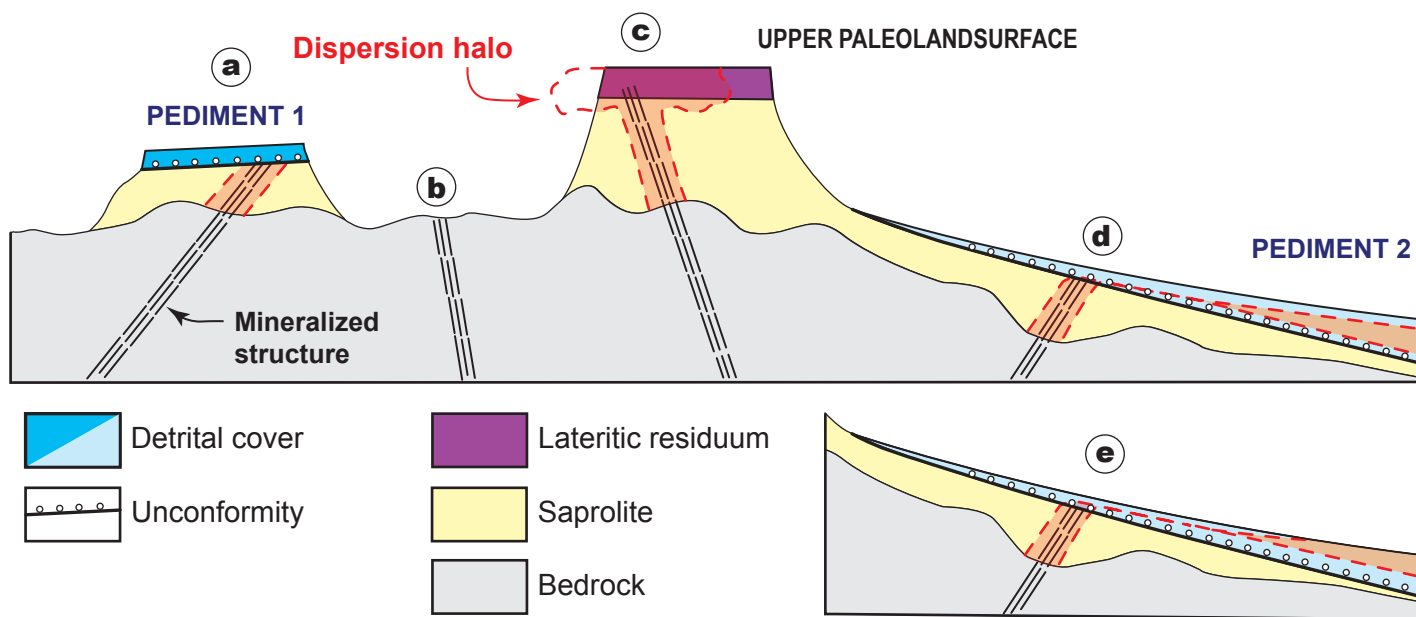
Sawadogo et al. Figure 13



Sawadogo et al. Figure 14



Sawadogo et al. Figure 15



Sawadogo et al. Figure 16

IDEALIZED DISPERSION MODELS IN WEST AFRICAN GRANITE-GREENSTONE TERRAINS

